

Is it Really Negative? Evaluating Natural Language Video Localization Performance on Multiple Reliable Videos Pool

Nakyeong Yang¹, Minsung Kim¹, Seunghyun Yoon², Joongbo Shin³ and Kyomin Jung¹

¹Seoul National University, ²Adobe Research, ³LG AI Research

{yny0506, kms0805, kjung}@snu.ac.kr
syoona@adobe.com, jb.shin@lgresearch.ai

Abstract

With the explosion of multimedia content in recent years, Video Corpus Moment Retrieval (VCMR), which aims to detect a video moment that matches a given natural language query from multiple videos, has become a critical problem. However, existing VCMR studies have a significant limitation since they have regarded all videos not paired with a specific query as negative, neglecting the possibility of including false negatives when constructing the negative video set. In this paper, we propose an **MVMR** (Massive Videos Moment Retrieval) task that aims to localize video frames within a massive video set, mitigating the possibility of falsely distinguishing positive and negative videos. For this task, we suggest an automatic dataset construction framework by employing textual and visual semantic matching evaluation methods on the existing video moment search datasets and introduce three MVMR datasets. To solve MVMR task, we further propose a strong method, CroCs, which employs cross-directional contrastive learning that selectively identifies the reliable and informative negatives, enhancing the robustness of a model on MVMR task. Experimental results on the introduced datasets reveal that existing video moment search models are easily distracted by negative video frames, whereas our model shows significant performance.¹

1 Introduction

Enabled by the increased accessibility of video-sharing platforms along with the advancement of networking and storage technology, a vast number of new content is available on the web daily. With this huge number of contents, Natural Language Video Localization (NLVL) task, searching for a video moment suitable for a given query, has emerged as an essential problem (Anne Hendricks et al., 2017; Gao et al., 2017). However, this line of

¹We have opened an anonymous GitHub page to make our code and dataset publicly available: [link](#)

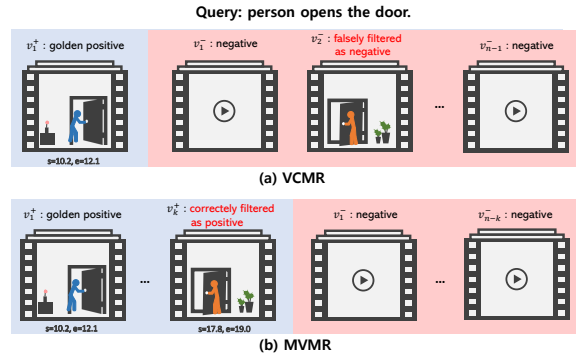


Figure 1: **MVMR vs. VCMR**. In existing VCMR studies, only a single golden positive video moment is identified as positive, while entire videos not paired with a specific query are regarded as negative. Our proposed MVMR filters positive video moments for a query from the whole video set; thus, it covers more practical and generalized use cases with reliable settings. v_i^+ and v_j^- mean a positive and a negative video, respectively.

research narrows down the task to an impractical setting by targeting the search over a single video; thus, it bears limitations in retrieving relevant information over whole media pools. Therefore, Video Corpus Moment Retrieval (VCMR) task that retrieves a correct positive moment among numerous negative videos has emerged (Escorcía et al., 2019; Lei et al., 2020; Ma and Ngo, 2022; Jung et al., 2022). Nonetheless, VCMR also has significant limitations as it merely extends NLVL datasets by categorizing all unpaired moments for a specific text query as negative. This assumption diverges from the practical setting of video moment search where multiple positive videos exist in whole media collections. Furthermore, existing VCMR studies have overlooked the potential presence of false-negative videos within the unpaired video set when constructing video retrieval pools for a specific query. As a result, evaluating the performance of NLVL models using an existing VCMR framework may lead to unreliable results. For example, in TACoS test dataset, it is noteworthy that the number of videos with queries exactly matching the

text "The person gets out a knife." amounts to 60% of all the videos. It is a significant problem since more videos will likely be incorrectly classified as negatives when expanding the matching criteria to include broader semantic similarities.

To bridge these gaps, we propose an **MVMR** (**M**assive **V**ideos **M**oment **R**etrieval) task, which expands the search coverage to a massive video set that can include any number of positive videos as shown in Figure 1. Specifically, given a query q with a positive videos v_1^+, \dots, v_k^+ and a negative videos v_1^-, \dots, v_{n-k}^- , the MVMR task aims to detect temporal moments in the positive videos that matches the query from a massive video set $V_q^{+,-} = \{v_1^+, \dots, v_k^+, v_1^-, \dots, v_{n-k}^-\}$. Furthermore, we propose simple and effective methods to construct a practical MVMR dataset by leveraging publicly available NLVL datasets. A critical challenge in converting an NLVL dataset into an MVMR dataset is accurately defining positive and negative videos for each query. However, manually performing this task by humans is exceedingly labor-intensive due to the massive volume of videos that need to be evaluated for each query. To address this issue, we propose an automated framework for MVMR dataset construction. This framework employs textual and visual semantic matching evaluation methods to define MVMR positive and negative videos while mitigating the danger of false categorization. Specifically, we examine the similarity between a target query and all videos in an NLVL dataset using SimCSE (Gao et al., 2021) and EMScore (Shi et al., 2022) models to define a massive video set. To this end, we construct three MVMR datasets, and we confirm that three samples of the introduced datasets contain only 1.5%, 0.2%, and 3.5% falsely defined videos, showing that our approach successfully creates a practical benchmark dataset from human evaluation.

To tackle MVMR task, we also introduce a novel negative sample training method, **C**ross-directional **H**ard and **R**eliable **N**egative **C**ontrastive **L**earning (CroCs). Specifically, CroCs adopts two training mechanisms: (1) weakly-supervised potential negative learning by assessing the similarity between queries, and (2) hard-negative learning by utilizing the relevance score between queries and moments predicted by a model, which helps find challenging negative samples. We demonstrate the performance of strong baseline models, including a state-of-the-art model, to compare with our model

in the new scenario (MVMR). The experimental results show that the performance of baseline models significantly degrades on the new task. For example, the state-of-the-art model, MMN, shows average 29.7% degradation on R@1 (IOU0.5) for all MVMR datasets, revealing the difficulty of the MVMR task. In contrast, our CroCs outperforms baseline models significantly in the MVMR setting, and this result proves that informative negative samples enhance the performance of the MVMR task. Moreover, we solve the MVMR task in a more practical scenario by adopting a pipeline with a video retrieval model, revealing that CroCs also outperforms the strong baseline.

2 Backgrounds

2.1 Natural Language Video Localization

Natural language video localization (NLVL), which aims to detect a specific moment in a video that matches a given text query, is one of the most challenging problems in the video-language multi-modal domain (Zhang et al., 2020b,a; Nan et al., 2021; Gao and Xu, 2021; Liu et al., 2021; Wang et al., 2022). Therefore, the NLVL task has been explored extensively, with numerous effective methods emerging. Some novel approaches have regarded the problem as question-answering (QA) tasks (Seo et al., 2018; Joshi et al., 2020), by leveraging a QA model to encode a multi-modal representation and then predicting the frames that correspond to the start and end of the moment that match a query (Ghosh et al., 2019; Zhang et al., 2020a). However, NLVL studies operate within an impractical framework, focusing on searching within a single video. Consequently, they have limitations in retrieving relevant information across the whole media repositories.

2.2 Video Corpus Moment Retrieval

Existing studies (Escorcia et al., 2019; Lei et al., 2020; Ma and Ngo, 2022; Jung et al., 2022) have tried to extend the NLVL to search on multiple video pools, naming it the Video Corpus Moment Retrieval (VCMR) task, which focuses on retrieving a moment from multiple videos for a given query. However, the VCMR simply extends the NLVL task by designating only one matched positive video moment for a target query as a positive, while labeling all unmatched videos as negative videos. This approach deviates from the practical scenario of the video moment search since multiple

Dataset	# Queries / # Videos	Avg Len (sec) Moment / Video	Avg # Moments per Query	Avg Query Len	# Max Positive / # Retrieval Pool
Charades-STA	3720 / 1334	7.83 / 29.48	1	6.24	1 / 1
ActivityNet	17031 / 4885	40.25 / 118.20	1	12.02	1 / 1
TACoS	4083 / 25	31.87 / 367.15	1	8.53	1 / 1
MVMR _{Charades-STA}	3716 / 1334	7.83 / 29.48	3.07	6.23	5 / 50
MVMR _{ActivityNet}	16941 / 4885	40.32 / 118.20	1.11	12.03	5 / 50
MVMR _{TACoS}	2055 / 25	28.55 / 367.15	2.24	7.31	5 / 5

Table 1: **Summary of datasets.** Remarkably, the queries of MVMR_{Charades-STA} and MVMR_{TACoS} generally include multiple positive moments, and it proves that existing VCMR studies are exposed to the risk of false negatives.

positive videos can be present for a target query. Moreover, existing VCMR studies have failed to consider the possibility of false-negative when constructing the negative video set for a specific query, which poses a significant reliability issue.

3 Problem Definition

MVMR task evaluates video moment retrieval models under an MVMR dataset with k positive videos and $n - k$ negative videos for each query. Given a positive video set $V_q^+ = \{v_1^+, \dots, v_k^+\}$ and a negative video set $V_q^- = \{v_1^-, \dots, v_{n-k}^-\}$, the MVMR task aims to localize a moment (x_s, x_e) of a specific video v that matches the query from massive video set $V_q^{+,-} = \{v_1^+, \dots, v_k^+, v_1^-, \dots, v_{n-k}^-\}$, where x_s and x_e mean start and end points of the moment, respectively. In MVMR task, we aim to retrieve an optimal positive moment (x_s^*, x_e^*) that matches semantically with the text query q . We derive confidence scores of moments for the whole n massive videos and select the moment with the highest score as a prediction.

4 MVMR Dataset Construction

Our MVMR setting automatically reconstructs an NLVL dataset by expanding it to associate each query with multiple positive and negative moments. The paired positive and negative videos are carefully selected with semantic similarity check techniques. In the following, we detail our process for constructing an MVMR dataset and present the analyses of the three constructed MVMR datasets.

4.1 Semantic Similarity Check

This section examines the similarity between a target query q and a video v using semantic text embedding and video captioning evaluation models.

Query Similarity-based Check. NLVL datasets consist of video set $V = \{v_1, \dots, v_l\}$ and paired query set $Q_v = \{q_1, \dots, q_m\}$ for each video v , where l and m is the number of videos and text

queries included in a dataset, respectively. Since each text query semantically describes the paired moment, we use queries to obtain semantic information about the paired video. For example, suppose that a video v is paired with a query q , "*The person gets out a knife*", in a moment (x_s, x_e) . Since a target query \hat{q} , "*The person takes out a knife*", is highly similar to the query q , \hat{q} is associated with the moment (x_s, x_e) of the video v . We use a semantic text embedding model, SimCSE (Gao et al., 2021), to distinguish positive and negative videos for each query. Specifically, we first obtain embeddings $e_{\hat{q}}$ and e_{q_1}, \dots, e_{q_m} for the target text query \hat{q} and all video text queries q_1, \dots, q_m using SimCSE, respectively. We calculate cosine similarity $s_{te}(\hat{q}, q_i)$ between $e_{\hat{q}}$ and e_{q_i} to quantify the semantic matching, and select the maximum similarity among $s_{te}(\hat{q}, q_1), \dots, s_{te}(\hat{q}, q_m)$ to use it as the query-video matching score $s_{te}(\hat{q}, v)$ of the target query \hat{q} and the video v . We select *max aggregation* to obtain $s_{te}(\hat{q}, v)$ since the video should be regarded as a positive video, even if only one similar query to a target query exists in a video.

Query-video Similarity-based Check. Queries associated with a video may describe the video limitedly since they may not cover all of its context. Therefore, we examine a visual semantic matching between a query and a video to filter positive and negative videos. We use EMScore (Shi et al., 2022), a video captioning evaluation model, to quantify the visual semantic similarity s_{tv} , used as a complementary filtering method on videos primarily filtered through the query similarity s_{te} .

4.2 Distinguishing Positive and Negative

This section describes constructing positive and negative video sets using the calculated query-video similarity, s_{te} and s_{tv} . Positive candidates are distinguished by primarily excluding videos $s_{te}(q, v) < t_{te}^+$, where t_{te}^+ is a hyper-parameter. We further exclude videos that have lower similarity

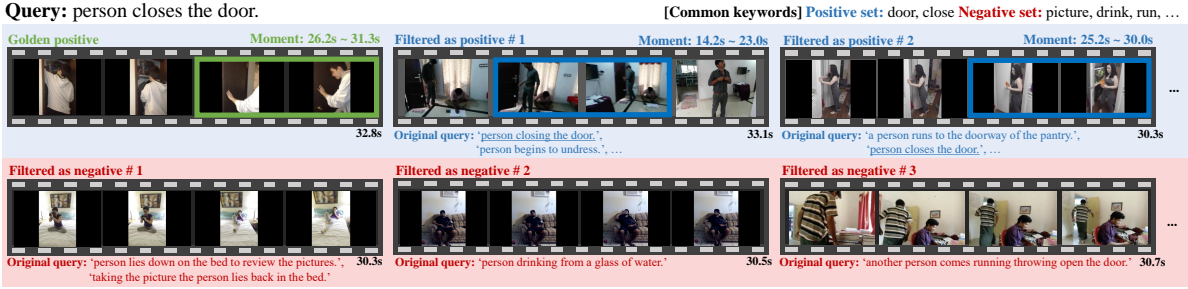


Figure 2: **Examples of constructed MVMR datasets.** We visualize positive and negative video sets for the query “person closes the door” of the MVMR_{Charades-STA}. A green solid box means a golden positive moment, and blue solid boxes show moments assigned to videos classified as positive. The underlined queries mean the most similar query described in Section 4.1 (*max aggregation*).

than the mean s_{tv} of all golden positive query-video pairs (q, v^*) for all queries. We construct final MVMR positives by randomly sampling k videos from this filtered set of positive candidates. Negative candidates are defined by excluding videos with $s_{te}(q, v) > t_{te}^-$, where t_{te}^- is also a hyper-parameter. We additionally exclude videos that have higher similarity than the mean s_{tv} of query-video pairs (q, v^-) , which are primarily filtered as negatives using s_{te} . Like MVMR positives, we construct final MVMR negatives by randomly sampling $(n - k)$ videos from this set of negative candidates. From this process, a total of n videos retrieval pool $V_q^{+, -} = \{v_1^+, \dots, v_k^+, v_1^-, \dots, v_{n-k}^-\}$ is obtained for each query.

5 MVMR Dataset Analysis

5.1 MVMR Settings.

This section describes the used NLVL datasets and detailed settings to derive MVMR positive and negative candidates using SimCSE and EMScore.

NLVL Datasets. We extend widely-used NLVL datasets (Charades-STA (Gao et al., 2017), ActivityNet (Krishna et al., 2017), and TACoS (Regneri et al., 2013)) to construct three MVMR evaluation datasets, and name the constructed datasets as MVMR_{DATASOURCE}. Each NLVL dataset consists of multiple videos with query-moment pairs. The details of each NLVL dataset are shown in Appendix A.

Filtering Settings. We use STS16 dataset (Agirre et al., 2016) to empirically validate varying SimCSE filtering hyper-parameters, t_{te}^+ and t_{te}^- . The dataset provides text pairs and human-annotated similarity scores (five-point Likert scale); two texts are regarded as similar when the score is higher than 3. We analyze the distribution of

SimCSE and human annotated scores for all text pairs in the dataset, and select $t_{te}^+ = 0.9$ to derive MVMR positive candidates since it is regarded as the best threshold to distinguish similar queries. We also select $t_{te}^- = 0.5$ to filter MVMR negative candidates. The distribution of SimCSE and human-annotated scores are shown in Appendix B.

5.2 MVMR Analysis

We set a video retrieval pool as n , containing at most k positive videos for each query. If the number of MVMR positive candidates derived for each query is less than k , we include all positive candidates as positive samples. Also, if the total number of MVMR positive and MVMR negative candidates for a query is less than n , the query is excluded from the final MVMR dataset.

Datasets Statistic. We set the number of videos in the MVMR_{Charades-STA} and the MVMR_{ActivityNet} retrieval pools as $n = 50$, and the maximum number of positive moments per query k is set to 5. The former consists of 3,716 queries for 1,334 videos, each containing an average of 3.07 positive moments. The latter contains 16,941 queries for 4,885 videos, each including an average of 1.11 positive videos. We set the number of videos for the MVMR_{TACoS} and the maximum number of positive moments per query as 5 and 5, respectively, since TACoS test set contains only 25 videos. It includes 2,055 queries for 25 videos, each containing an average of 2.24 positive videos. The summary of the MVMR datasets is shown in Table 1.

Dataset Quality. Figure 2 shows filtered positive and negative examples for a query of the constructed MVMR_{Charades-STA} dataset. The figure indicates that similar videos to a query are correctly classified as positive. Appendix D shows more examples of collected positives and negatives for

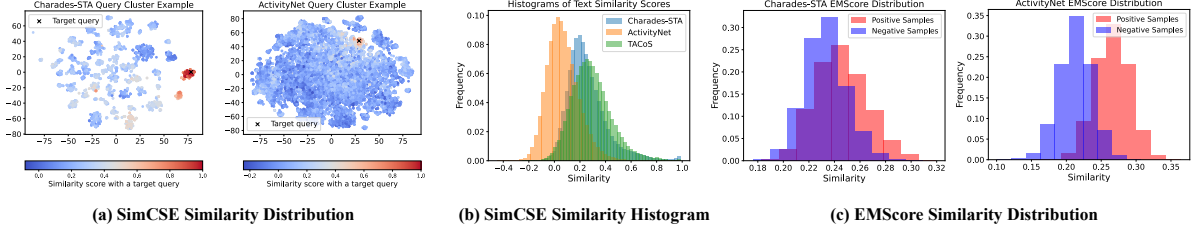


Figure 3: **Qualitative Analysis for Filtering Methods.** We visualize the derived similarity scores of SimCSE and EMScore to verify the constructed MVMR datasets. We use T-SNE to reduce the dimension of each query embedding for displaying each query (dot) of SimCSE Similarity Distribution.

three MVMR datasets.

Figure 4 shows the keyword cohesiveness of positive and negative sets about the MVMR_{Charades-STA} and MVMR_{ActivityNet} datasets. We quantify the cohesiveness of the MVMR positive and negative sets by examining the original queries paired with all videos in each set. If paired queries are similar, the video set is regarded as well-clustered. Therefore, we measure the ratio of whether a word in an original query is included in an original query set of all other videos (co-occurrence ratio) for the positive set and the negative set, respectively. Consequently, similar words are observed more frequently in the positive than negative set, revealing the cohesiveness of the MVMR positive set.

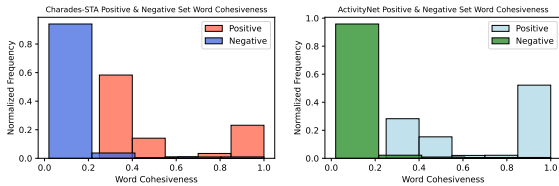


Figure 4: **Cohesiveness of the Positive and Negative sets.** The X and Y axes mean the word co-occurrence ratio and its frequency, respectively. The closer the word’s co-occurrence ratio approaches 1.0, the more cohesive it is.

Human Evaluation. We recruit crowd workers and ask them to examine 100 queries manually and their paired videos (by our method) and answer whether they are correctly labeled. Overall, we analyze 4,900, 4,900, and 400 videos for Charades-STA, ActivityNet, and TACoS, respectively, since each MVMR dataset consists of 49, 49, and 4 newly added videos (either positive or negative samples). The original video (i.e., golden positive sample) is excluded from this investigation. From human evaluation, we confirm that the newly introduced dataset contains only 1.5%, 0.2%, and 3.5% falsely categorized videos for the three datasets, respectively. TACoS exhibits a relatively higher query-relevant video ratio than the other two datasets since its test set includes only 25 videos

and consists of considerably similar cooking activities within the kitchen.

Analysis on Semantic Filtering Methods. We visualize the scores derived using SimCSE and EMScore to analyze our MVMR datasets qualitatively. Figure 3-(a) displays SimCSE embeddings of all queries in each dataset, illustrating the similarity between all queries and a specific target query, “*person turn a light on.*” (left) and “*He is using a push mower to mow the grass.*” (right). The figure of TACoS can also be found in Appendix B. The figures show that queries exhibit well-defined clusters for Charades-STA and TACoS, revealing the effectiveness of our query similarity-based filtering. These results are also supported by Figure 3-(b) SimCSE score histogram, showing that Charades-STA and TACoS have many similar queries. Figure 3-(c) illustrates histograms of EMScore similarity between queries and videos. The red and blue histograms correspond to the EMScore distribution of positive and negative samples, respectively. For the ActivityNet, EMScore effectively distinguishes positives and negatives. This success is attributed to that ActivityNet includes detailed queries and videos with diverse features. According to the findings presented in this section, the filtering method’s efficacy varies depending on the dataset’s characteristics. Consequently, a combination of two filtering methods (i.g., SimCSE and EMScore) should be employed in a complementary manner to ensure the construction of a reliable MVMR dataset.

6 Methods: CroCs

This section introduces a novel contrastive learning method, **CroCs**, which stands for **Cross-directional Hard and Reliable Negative Contrastive Learning**, to solve the MVMR task. A key challenge in solving the MVMR task is distinguishing positives from multiple negative distractors. Therefore, we select MMN (Wang et al., 2022) since it is the optimal baseline model for the MVMR task as it uses

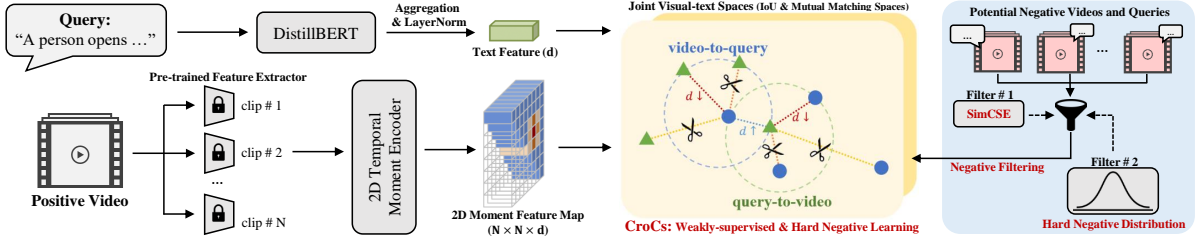


Figure 5: **CroCs Overview.** We adopt informative negative contrastive learning to solve the MVMR task. The dots and triangles are the features of moments and texts. The blue dash lines are matched moment-text pairs to be pulled in, while the red dash lines are negative samples of intra/inter-video to be pushed away. The yellow and orange dash lines are unmatched moment-text pairs, but not to train by filtering out since they are easy and false-negatives.

contrastive learning to distinguish negative samples from positives effectively. We use the MMN as the backbone of our model and enhance its ability by applying CroCs in training procedures to solve the challenge in the MVMR task. MMN has limitations in neglecting the potential presence of false-negative video moments since it regards all randomly selected in-batch samples as negatives in contrastive learning. Furthermore, it overlooks the importance gap among negative samples. Our CroCs solves these two limitations of the MMN by adopting two contrastive learning procedures: (1) Weakly-supervised potential negative learning and (2) Informative hard-negative learning.

6.1 Weakly-supervised Contrastive Learning

A critical consideration in the contrastive learning framework is the potential presence of false-negatives. This issue arises when all videos, except for the golden video, are categorized as negative training samples. To mitigate this concern, we propose excluding false-negative videos to refine the contrastive learning process. Specifically, we adopt the SimCSE filtering to identify and exclude false-negative videos as follows:

$$V_{tr}^-(q) = \{v | s_{te}(q, v) < t_{tr}\}, \quad \forall v \in V \quad (1)$$

where $V_{tr}^-(q)$ is a negative sample set of a specific query q to use during the contrastive learning procedure. $s_{te}(q, v)$ is query-video similarity described in Section 4.1. t_{tr} is a hyper-parameter for SimCSE score filtering. If a specific video shows a value of $s_{te}(q, v)$ above the threshold t_{tr} for target query q , we classify v as false-negative for q . Therefore, we exclude v in negative samples of contrastive learning for q .

6.2 Hard-negatives Contrastive Learning

Easy or false-negatives may distract a model from learning proper knowledge during the training pro-

cess. Inspired by recent progress in using hard-negative sampling for the document retrieval task (Zhou et al., 2022), we categorize negatives according to the matching score between a target query and negative moments as follows: (1) Negatives that are clearly irrelevant and have low matching scores should be sampled less frequently (Easy-negative); (2) Negatives that are highly relevant and have high matching scores should also be sampled less frequently (False-negative); (3) Negatives that are uncertain and have matching scores similar to true-positives should be sampled more frequently since they provide useful information (Hard-negative). Based on these criteria, we distinguish hard-negative samples and adopt a retraining process for a model already trained on a specific dataset using only hard-negative samples. We define the negative moments and query sampling distribution as follows:

$$\begin{aligned} p'(m|q) &\propto \exp(-(r(q, m) - \bar{r}(q, m^+))^2), \quad \forall m \in M_q^- \quad (2) \\ p'(q|m) &\propto \exp(-(r(q, m) - \bar{r}(q^+, m))^2), \quad \forall q \in Q_m^- \end{aligned}$$

where $r(q, m)$ is a matching score between a query and a moment calculated using the already trained video moment retrieval model, and $\bar{r}(q, m^+)$ and $\bar{r}(q^+, m)$ is mean matching scores for all golden positive moments and queries, respectively. M_q^- and Q_m^- is potential negative candidates for a query q and a moment m , respectively. $p'(m|q)$ means the probability that moment m is sampled as negative when given query q . Therefore, negative candidate moments with a close distance to the average matching score of golden query-moment pairs have a high sampling probability. Likewise, $p'(q|m)$ means the probability that query q is sampled as negative when given moment m . We also reformulate $p'(m|q)$ to $p'(v|q)$ for computational efficiency in a sampling procedure as follows:

$$\begin{aligned} r(q, v) &= \max(\{r(q, m_1), \dots, r(q, m_i)\}), \quad \forall m_i \in v \\ p'(v|q) &\propto \exp(-(r(q, v) - \bar{r}(q, v^+))^2), \quad \forall v \in V_q^- \quad (3) \end{aligned}$$

$p'(q|v)$ can be formulated similarly by calculating \bar{r} about positive queries for each video.

6.3 Reliable Mutual Matching Network

This section describes a model architecture to apply the proposed contrastive learning method, CroCs. We adopt a bi-encoder architecture with a late modality fusion by an inner product in the joint visual-text representational space following the baseline MMN. By adopting a bi-encoder architecture, we can efficiently search for moments with pre-calculated video moment representations given a user query. Our whole model architecture is shown in Figure 5. Our model represents each query and video moment using query and video encoders to two joint visual-text spaces (IoU and mutual matching spaces). From the joint visual-text space, we compute the matching score between the query and video moment representations and select the best video moment. The details of the model architecture are described in the appendix C.1.

We select the binary cross entropy and contrastive learning losses and train our model following two steps: (1) the first training step using the two loss functions (binary cross entropy and contrastive learning losses) filtering out false-negatives described in Section 6.1; (2) the second training step using two loss functions with only hard-negatives described in Section 6.2. To calculate the similarity between the text and video moment features projected in the IoU space, we compute the cosine similarity s^{iou} . To adjust the range of the final prediction, we multiply the cosine similarity by a factor of 10, following the MMN. This amplification results in the final prediction $p_i^{iou} = \sigma(10 \cdot s_i^{iou})$, where σ represents the sigmoid function. The binary cross-entropy loss is then calculated as follows:

$$L_{bce} = -\frac{1}{C} \sum_{i=1}^C (y_i \log p_i^{iou} + (1 - y_i) \log (1 - p_i^{iou})) \quad (4)$$

where p_i^{iou} is the confidence score of each moment, and C is the total number of valid candidates. We calculate L_{bce} for positive and true-negative samples derived in Section 6.1.

We use the cross-directional contrastive learning loss to effectively train the model using the informative negatives derived from the methods described in Section 6.1 and 6.2. The mutual matching contrastive learning loss considering the informative negative samples selection process is as follows:

$$\begin{aligned} p^*(q_i|m) &= \frac{\exp((f_i^{qT} f^m - \psi)/\tau_m)}{\exp((f_i^{qT} f^m - \psi)/\tau_m) + \sum_{j \in \mathcal{I}_m^-} \exp(f_j^{qT} f^m / \tau_m)} \\ p^*(m_i|q) &= \frac{\exp((f_i^{mT} f^q - \psi)/\tau_q)}{\exp((f_i^{mT} f^q - \psi)/\tau_q) + \sum_{j \in \mathcal{I}_q^-} \exp(f_j^{mT} f^q / \tau_q)} \\ L_{rmm} &= -\left(\sum_{i=1}^N (\log p^*(i_m|q_i)) + \sum_{i=1}^N (\log p^*(i_q|m_i)) \right) \end{aligned} \quad (5)$$

where q_i and m_i are corresponding positive query and moment for each moment and query, respectively. f^m and f^q are the moment and query features in the joint visual-text space. τ_q and τ_m are temperatures. \mathcal{I}^- means the indices of informative negatives derived using our sampling methods.

The final loss, denoted as L , is formulated as a linear combination of the binary cross-entropy loss and the reliable mutual matching loss. The matching score s , for a specific moment given the text query, is obtained by multiplying the iou score s^{iou} with the reliable mutual matching score s^{rmm} . The reliable mutual matching score is calculated for the features in the mutual matching space in the same way as the iou score.

$$L = L_{bce} + \lambda L_{rmm}, \quad s = s^{iou} \cdot s^{rmm} \quad (6)$$

7 Experiments

7.1 Experimental Settings

This section describes the experimental settings of the CroCs and other baselines. More details are shown in Appendix C.

Implementation Details. We use standard off-the-shelf video feature extractors without any fine-tuning: VGG (Simonyan and Zisserman, 2015) feature for Charades-STA; C3D (Tran et al., 2015) feature for ActivityNet and TACoS following (Wang et al., 2022). We set the filtering hyper-parameter as $t_{tr} = 0.9$ for the weakly-supervised contrastive learning. We choose the number of the CroCs hard negative samples to calculate $p'(q|v)$ as 100, 200, and 100 and $p'(v|q)$ as 50, 100, and 5 for Charades-STA, ActivityNet, and TACoS, respectively. These hyper-parameters are chosen from varying parameter setting experiments as shown in Figure 8. In the hard-negative fine-tuning stage, the learning rates are degraded by multiplying 0.1.

Baselines. We first select the state-of-the-art models, MMN (Wang et al., 2022) and G2L (Li et al., 2023), as strong baselines. As the MVMR task can be formulated as an open-domain question answering (QA) task, we fur-

Dataset	Model	R@1	R@1	R@1	R@5	R@5	R@5	R@20	R@20	R@20	R@50	R@50	R@50
		IOU0.3	IOU0.5	IOU0.7	IOU0.3	IOU0.5	IOU0.7	IOU0.3	IOU0.5	IOU0.7	IOU0.3	IOU0.5	IOU0.7
MVMR _{Charades-STA}	CET	3.96	2.96	2.02	15.34	11.79	6.97	39.85	32.21	19.91	59.58	50.54	33.88
	BET	4.57	2.99	1.94	14.26	10.98	7.00	31.05	25.11	16.55	45.88	37.86	26.08
	G2L	4.30	2.78	1.97	14.34	10.59	7.36	40.89	34.74	21.33	71.92	62.72	44.82
	MMN	13.99	12.78	8.40	37.86	33.29	22.36	64.80	57.83	41.71	80.11	73.09	56.75
	CroCs [†]	<u>18.38</u>	<u>16.31</u>	<u>10.76</u>	43.86	39.05	<u>26.99</u>	69.48	62.89	<u>46.39</u>	<u>82.88</u>	<u>76.08</u>	<u>60.28</u>
	CroCs	19.27	17.38	11.44	<u>43.54</u>	<u>39.02</u>	27.91	<u>68.08</u>	<u>60.98</u>	46.39	82.99	76.29	60.76
MVMR _{ActivityNet}	CET	1.26	0.90	0.56	2.81	2.32	1.75	5.41	4.73	3.87	8.97	8.02	6.56
	BET	1.56	1.16	0.76	3.02	2.55	2.03	5.30	4.64	3.80	8.13	7.10	5.88
	G2L	1.66	1.32	0.96	7.82	6.43	4.55	26.84	21.66	14.81	62.99	50.07	32.99
	MMN	13.82	10.71	6.93	31.54	25.04	16.55	54.79	44.50	30.62	73.08	62.09	45.76
	CroCs [†]	<u>16.46</u>	<u>12.68</u>	<u>7.87</u>	<u>36.03</u>	<u>28.47</u>	<u>18.16</u>	<u>57.91</u>	<u>46.52</u>	<u>31.12</u>	<u>73.82</u>	<u>62.12</u>	44.89
	CroCs	20.63	15.58	9.51	44.13	34.70	22.40	67.01	55.58	38.55	79.91	70.02	53.20
MVMR _{TACoS}	CET	8.95	5.79	3.89	26.18	18.88	12.17	54.84	42.53	23.70	-	-	-
	BET	8.22	5.30	2.97	29.46	14.84	8.32	55.67	39.76	21.51	-	-	-
	G2L	8.72	5.82	4.31	30.61	21.51	12.29	56.52	42.35	22.52	-	-	-
	MMN	10.56	8.61	5.60	36.16	25.84	15.47	58.20	43.89	23.80	-	-	-
	CroCs [†]	13.43	<u>10.75</u>	<u>6.76</u>	<u>36.45</u>	<u>27.01</u>	<u>15.28</u>	<u>58.30</u>	<u>44.38</u>	25.16	-	-	-
	CroCs	<u>13.24</u>	10.75	7.30	39.22	29.68	16.50	60.05	44.77	<u>24.62</u>	-	-	-

Table 2: **Experimental Results on MVMR datasets.** Bolded and under-lined results indicate the 1st and 2nd best performance, respectively. CroCs[†] is the model using only weakly-supervised contrastive learning (§6.1). CroCs uses both of two contrastive learning methods (§6.1 and §6.2). We train all the baselines as three trials and report the averaged MVMR scores.

ther choose two types of QA models that employ a cross-encoder architecture (i.e., Cross-Encoder Transformer) and a dual-encoder architecture (i.e., Bi-Encoder Transformer), respectively. These architectures are widely adopted in existing NLVL tasks (Zhang et al., 2020b; Gao and Xu, 2021) due to the closeness of the two tasks.

Evaluation Metrics. We evaluate baselines by calculating Rank n@m. It is defined as the percentage of queries having at least one correctly retrieved moment, i.e., $\text{IoU} \geq m$, in the top- n derived moments. The existing NLVL studies have reported the results of $m \in \{0.3, 0.5, 0.7\}$ with $n \in \{1, 5\}$ (Wang et al., 2022). But, since our MVMR setting searches for massive videos, we report the extended results as $m \in \{0.3, 0.5, 0.7\}$ with $n \in \{1, 5, 20, 50\}$ for Charades-STA and AcitivityNet and $m \in \{0.3, 0.5, 0.7\}$ with $n \in \{1, 5, 20\}$ for TACoS.

7.2 MVMR Results

MVMR Performance. We evaluate the performance of CroCs and the baseline models on the introduced MVMR datasets. Table 2 shows the experimental results of CroCs and other baselines for our MVMR task. Surprisingly, although CET and BET show quite strong performance on the NLVL task, their performance on the MVMR task notably drops. For examples, CET and MMN show average 34.5 and 29.7 degradation on R@1(IOU.5) for all MVMR datasets. These outcomes indicate

that the current NLVL task performance alone is not enough to verify that a model is well-trained. We reveal that CroCs outperforms all other baselines on MVMR task, and this suggests that our model correctly discriminates features of negative and positive moments. Experiments show that the models on Charades-STA and TACoS significantly improve performance from the weakly-supervised learning since similar queries exist frequently in these datasets and the possibility of false-negatives is high. However, the performance of ActivityNet is attributed to the hard-negative learning since it includes various and complex text queries.

MVMR Settings with Video Retrieval. The practical usage scenario for the MVMR should include video retrieval. Therefore, We also conduct MVMR experiments with a video retrieval model, PRMR model (Dong et al., 2022), shown as Table 3. We construct a pipeline to filter top-5 logit videos from our MVMR retrieval pool using the PRMR model and solve MVMR task. We use the publicly deployed PRMR model on Charades-STA and ActivityNet datasets. These experiments prove that video retrieval models are helpful to increase MVMR performance, and CroCs still shows superior performance than MMN in this pipeline.

Model	R@1 IOU0.3	R@1 IOU0.5	R@5 IOU0.3	R@5 IOU0.5
MMN _{Charades-STA}	32.15	27.10	65.97	57.66
CroCs _{Charades-STA}	36.64	29.27	68.06	59.78
MMN _{ActivityNet}	32.39	25.04	66.84	55.03
CroCs _{ActivityNet}	39.25	29.59	71.54	60.02

Table 3: **MVMR Experiments with Video Retrieval.**

8 Conclusion

In this paper, we propose the Massive Videos Moment Retrieval (MVMMR) task, which aims to detect a moment for a natural language query from a massive video set. To stimulate the research, we propose a simple automatic method to construct reliable MVMMR datasets and build three MVMMR datasets using existing NLVL datasets. We introduce a robust training method called CroCs to distinguish positives from negative distractors effectively in solving MVMMR task.

Limitations

Our dataset construction framework automatically defines positive and negative sets using semantic similarity evaluation. Unlike the existing VCMR framework, which overlooks the risk of labeling errors in its automated dataset construction process, our MVMMR framework introduces some filtering methods to mitigate labeling errors. However, our method still faces limitations due to its reliance on automatic labeling, which fundamentally carries a risk of labeling inaccuracies. To eliminate the risk of labeling errors thoroughly, a constructed dataset should be reviewed manually through complete enumeration.

References

- Eneko Agirre, Carmen Banea, Daniel Cer, Mona Diab, Aitor Gonzalez Agirre, Rada Mihalcea, German Rigau Claramunt, and Janyce Wiebe. 2016. Semeval-2016 task 1: Semantic textual similarity, monolingual and cross-lingual evaluation. In *SemEval-2016, 10th International Workshop on Semantic Evaluation; 2016 Jun 16-17; San Diego, CA. Stroudsburg (PA): ACL; 2016. p. 497-511*. ACL (Association for Computational Linguistics).
- Lisa Anne Hendricks, Oliver Wang, Eli Shechtman, Josef Sivic, Trevor Darrell, and Bryan Russell. 2017. Localizing moments in video with natural language. In *Proceedings of the IEEE international conference on computer vision*, pages 5803–5812.
- Jianfeng Dong, Xianke Chen, Minsong Zhang, Xun Yang, Shujie Chen, Xirong Li, and Xun Wang. 2022. Partially relevant video retrieval. In *Proceedings of the 30th ACM International Conference on Multimedia*, pages 246–257.
- Victor Escorcia, Mattia Soldan, Josef Sivic, Bernard Ghanem, and Bryan Russell. 2019. Temporal localization of moments in video collections with natural language.
- Jiyang Gao, Chen Sun, Zhenheng Yang, and Ram Nevatia. 2017. [TALL: temporal activity localization via language query](#). In *IEEE International Conference on Computer Vision, ICCV 2017, Venice, Italy, October 22-29, 2017*, pages 5277–5285. IEEE Computer Society.
- Junyu Gao and Changsheng Xu. 2021. Fast video moment retrieval. In *Proceedings of the IEEE/CVF International Conference on Computer Vision*, pages 1523–1532.
- Tianyu Gao, Xingcheng Yao, and Danqi Chen. 2021. Simcse: Simple contrastive learning of sentence embeddings. *arXiv preprint arXiv:2104.08821*.
- Soham Ghosh, Anuva Agarwal, Zarana Parekh, and Alexander Hauptmann. 2019. [Excl: Extractive clip localization using natural language descriptions](#).
- Fabian Caba Heilbron, Victor Escorcia, Bernard Ghanem, and Juan Carlos Niebles. 2015. [Activitynet: A large-scale video benchmark for human activity understanding](#). In *IEEE Conference on Computer Vision and Pattern Recognition, CVPR 2015, Boston, MA, USA, June 7-12, 2015*, pages 961–970. IEEE Computer Society.
- Mandar Joshi, Danqi Chen, Yinhan Liu, Daniel S. Weld, Luke Zettlemoyer, and Omer Levy. 2020. [Spanbert: Improving pre-training by representing and predicting spans](#).
- Minjoon Jung, Seongho Choi, Joochan Kim, Jin-Hwa Kim, and Byoung-Tak Zhang. 2022. Modal-specific pseudo query generation for video corpus moment retrieval. *arXiv preprint arXiv:2210.12617*.
- Ranjay Krishna, Kenji Hata, Frederic Ren, Li Fei-Fei, and Juan Carlos Niebles. 2017. [Dense-captioning events in videos](#). In *IEEE International Conference on Computer Vision, ICCV 2017, Venice, Italy, October 22-29, 2017*, pages 706–715. IEEE Computer Society.
- Jie Lei, Licheng Yu, Tamara L Berg, and Mohit Bansal. 2020. Tvr: A large-scale dataset for video-subtitle moment retrieval. In *Computer Vision—ECCV 2020: 16th European Conference, Glasgow, UK, August 23–28, 2020, Proceedings, Part XXI 16*, pages 447–463. Springer.
- Hongxiang Li, Meng Cao, Xuxin Cheng, Yaowei Li, Zhihong Zhu, and Yuexian Zou. 2023. G2l: Semantically aligned and uniform video grounding via geodesic and game theory. In *Proceedings of the IEEE/CVF International Conference on Computer Vision*, pages 12032–12042.
- Daizong Liu, Xiaoye Qu, Jianfeng Dong, Pan Zhou, Yu Cheng, Wei Wei, Zichuan Xu, and Yulai Xie. 2021. Context-aware biaffine localizing network for temporal sentence grounding. In *Proceedings of the IEEE/CVF Conference on Computer Vision and Pattern Recognition*, pages 11235–11244.

- Ilya Loshchilov and Frank Hutter. 2017. Decoupled weight decay regularization. *arXiv preprint arXiv:1711.05101*.
- Zhixin Ma and Chong Wah Ngo. 2022. Interactive video corpus moment retrieval using reinforcement learning. In *Proceedings of the 30th ACM International Conference on Multimedia*, pages 296–306.
- Guoshun Nan, Rui Qiao, Yao Xiao, Jun Liu, Sicong Leng, Hao Zhang, and Wei Lu. 2021. Interventional video grounding with dual contrastive learning. In *Proceedings of the IEEE/CVF conference on computer vision and pattern recognition*, pages 2765–2775.
- Michaela Regneri, Marcus Rohrbach, Dominikus Wetzel, Stefan Thater, Bernt Schiele, and Manfred Pinkal. 2013. [Grounding action descriptions in videos](#). *Transactions of the Association for Computational Linguistics*, 1:25–36.
- Victor Sanh, Lysandre Debut, Julien Chaumond, and Thomas Wolf. 2019. Distilbert, a distilled version of bert: smaller, faster, cheaper and lighter. *arXiv preprint arXiv:1910.01108*.
- Minjoon Seo, Aniruddha Kembhavi, Ali Farhadi, and Hannaneh Hajishirzi. 2018. [Bidirectional attention flow for machine comprehension](#).
- Yaya Shi, Xu Yang, Haiyang Xu, Chunfeng Yuan, Bing Li, Weiming Hu, and Zheng-Jun Zha. 2022. Emscore: Evaluating video captioning via coarse-grained and fine-grained embedding matching. In *Proceedings of the IEEE/CVF Conference on Computer Vision and Pattern Recognition*, pages 17929–17938.
- Gunnar A Sigurdsson, Gül Varol, Xiaolong Wang, Ali Farhadi, Ivan Laptev, and Abhinav Gupta. 2016. Hollywood in homes: Crowdsourcing data collection for activity understanding. In *European Conference on Computer Vision*, pages 510–526. Springer.
- Karen Simonyan and Andrew Zisserman. 2015. [Very deep convolutional networks for large-scale image recognition](#). In *3rd International Conference on Learning Representations, ICLR 2015, San Diego, CA, USA, May 7-9, 2015, Conference Track Proceedings*.
- Du Tran, Lubomir D. Bourdev, Rob Fergus, Lorenzo Torresani, and Manohar Paluri. 2015. [Learning spatiotemporal features with 3d convolutional networks](#). In *2015 IEEE International Conference on Computer Vision, ICCV 2015, Santiago, Chile, December 7-13, 2015*, pages 4489–4497. IEEE Computer Society.
- Zhenzhi Wang, Limin Wang, Tao Wu, Tianhao Li, and Gangshan Wu. 2022. Negative sample matters: A renaissance of metric learning for temporal grounding. In *Proceedings of the AAAI Conference on Artificial Intelligence*, volume 36, pages 2613–2623.
- Thomas Wolf, Lysandre Debut, Victor Sanh, Julien Chaumond, Clement Delangue, Anthony Moi, Pierric Cistac, Tim Rault, Rémi Louf, Morgan Funtowicz, et al. 2019. Huggingface’s transformers: State-of-the-art natural language processing. *arXiv preprint arXiv:1910.03771*.
- Hao Zhang, Aixin Sun, Wei Jing, and Joey Tianyi Zhou. 2020a. Span-based localizing network for natural language video localization. *arXiv preprint arXiv:2004.13931*.
- Songyang Zhang, Houwen Peng, Jianlong Fu, and Jiebo Luo. 2020b. [Learning 2d temporal adjacent networks for moment localization with natural language](#). In *The Thirty-Fourth AAAI Conference on Artificial Intelligence, AAAI 2020, The Thirty-Second Innovative Applications of Artificial Intelligence Conference, IAAI 2020, The Tenth AAAI Symposium on Educational Advances in Artificial Intelligence, EAAI 2020, New York, NY, USA, February 7-12, 2020*, pages 12870–12877. AAAI Press.
- Kun Zhou, Yeyun Gong, Xiao Liu, Wayne Xin Zhao, Yelong Shen, Anlei Dong, Jingwen Lu, Rangan Majumder, Ji-Rong Wen, Nan Duan, and Weizhu Chen. 2022. [Simans: Simple ambiguous negatives sampling for dense text retrieval](#).

A Datasets Details

Charades-STA is an extended dataset of action recognition and localization dataset Charades (Sigurdsson et al., 2016) by (Gao et al., 2017) for video moment retrieval. It is comprised of 5,338 videos and 12,408 query-moment pairs in the training set, and 1,334 videos and 3,720 query-moment pairs in the test set. We report evaluation results on test set in our experiments.

ActivityNet-Captions is constructed on ActivityNet v1.3 dataset (Heilbron et al., 2015), where included videos cover various complex human actions. It is originally designed for video captioning, and recently used into video moment retrieval. It contains 37,417, 17,505, and 17,031 query-moment pairs for training, validation, and testing respectively. We report the evaluation result on val_2 set following the setting of the MMN paper (Wang et al., 2022).

TACoS includes 127 videos selected from the MPII-Cooking dataset. It consists of 18,818 query-moment pairs of various cooking activities in the kitchen annotated by (Regneri et al., 2013). It (Gao et al., 2017) consists of 10,146, 4,589, and 4,083 query-moment pairs for training, validation and testing, respectively. We report evaluation results on test set in our experiments.

B Analysis on Filter Methods

We construct reliable MVMR datasets using SimCSE and EMScore. The visualizations of the similarity scores derived by SimCSE and EMScore is shown as Figure 7. For the SimCSE distribution, we select target queries of "person turn a light on", "The person peels a kiwi", and "He is using a push mower to mow the grass" for the Charades-STA, TACoS, and ActivityNet, respectively.

Figure 6 shows the distribution of SimCSE and human-annotated STS16 (Agirre et al., 2016) dataset scores. STS16 dataset provides text pairs and annotated similarity scores (five-point Likert scale). In the dataset, two texts are regarded as similar when the score is higher than 3. We visualize the distribution of SimCSE and human annotated scores for all text pairs in the dataset, and select $t_{te}^+ = 0.9$ and $t_{te}^- = 0.5$ as thresholds for the SimCSE filtering to derive MVMR positive and negative candidates, respectively. STS16 dataset includes text pairs that are challenging to distinguish. However, the three datasets utilized in our

experiment do not demand similarity measurement at such a complex level. Consequently, we can reliably discern the similarity between queries using the provided thresholds.

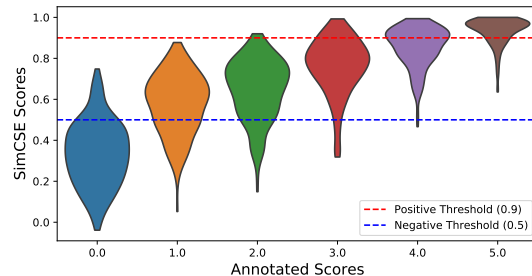


Figure 6: **The distribution of SimCSE and Human-annotated Scores.** The X and Y axes mean the human-annotated and the SimCSE scores, respectively. The width of each graph corresponds to the number of samples.

C Implementation Details

We use standard off-the-shelf video feature extractors without any fine-tuning. We use VGG (Simonyan and Zisserman, 2015) feature for Charades-STA and C3D (Tran et al., 2015) feature for ActivityNet and TACoS following the previous work (Wang et al., 2022). We train CroCs and MMN on 1 NVIDIA RTX A6000 GPU and early stop by averaging scores of all evaluation metrics.

C.1 CroCs

We implement CroCs by following MMN’s model architecture. CroCs represents each query and video moment using query and video encoders to a joint visual-text space. From the joint visual-text space, CroCs computes the similarity between the query and video moment representations and selects the best-matched video moment.

Query and Video Encoders. We choose DistilBERT (Sanh et al., 2019) for the text query encoder following MMN since it is a lightweight model showing significant performance. We calculate the representation of each query $f^q \in \mathbb{R}^d$ using the global average pooling over all tokens. We adopt the approach of encoding the input video as a 2D temporal moment feature map, inspired by 2D-TAN (Zhang et al., 2020b) and MMN. To achieve this, we segment the input video into video clips denoted as $\{c_i\}_{i=1}^{l_c/k}$, where each clip c_i consists of k frames. l_c means the total number of frames in the video. The clip-level representations are extracted

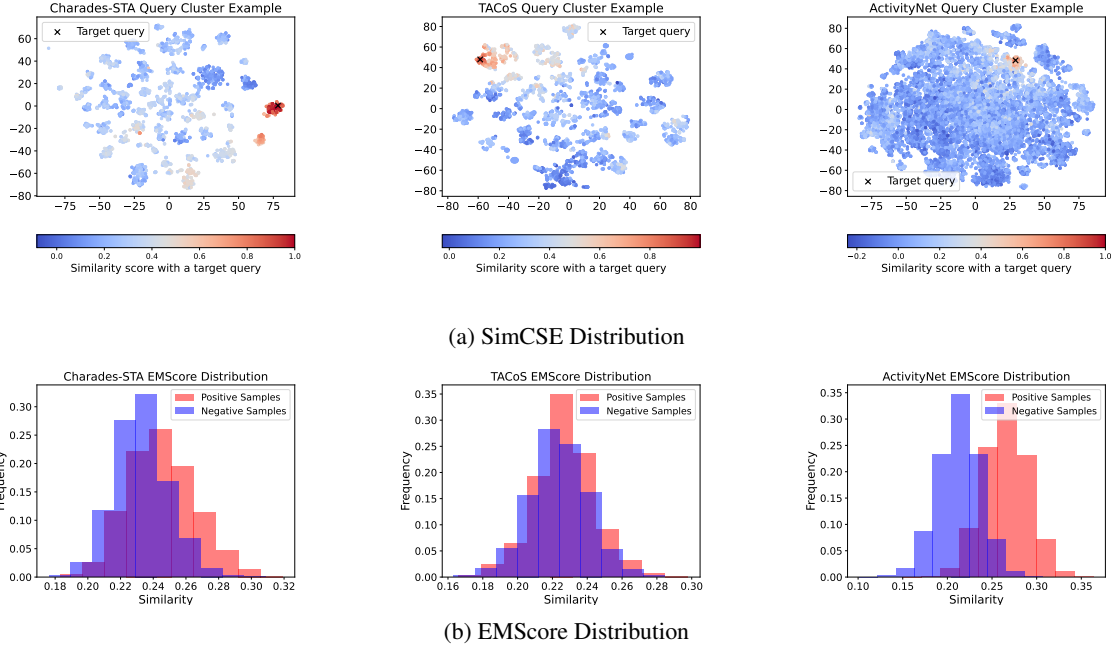


Figure 7: The Visualization of the SimCSE and EMScore Similarity Distribution.

using a pre-trained visual model (e.g., C3D). By sampling a fixed length with a stride of $\frac{l_c}{k \cdot N}$, we obtain N clip-level features. These features are then passed through an FC layer to reduce the dimensionality, resulting in the features $\{f_i^v\}_{i=1}^N$, where $f_i^v \in \mathbb{R}^d$. Utilizing these features, we construct a 2D temporal moment feature map $F \in \mathbb{R}^{N \times N \times d}$ by employing max-pooling as the moment-level feature aggregation method following the baseline (Wang et al., 2022). Additionally, we generate a 2D feature map F' of the same size by passing F to 2D Convolution, allowing the representation of moment relations as employed in MMN.

Joint Visual-Text Space. Initially, we apply layer normalization to both the video moments and text features. Subsequently, we utilize a linear projection layer and a 1×1 convolution layer to project the text and video in the same embedding space, respectively. The projected features are then employed in two distinct representational spaces: the IoU space and the mutual matching space. These spaces serve as the basis for computing the binary cross-entropy loss and the contrastive learning loss, respectively.

Hyperparameter Settings. Our convolution network for deriving 2D features is exactly the same as MMN, including the number of sampled clips N , the number of 2D conv layers L , kernel size, and channels. We set the dimension of the joint

feature visual-text space $d = 256$, and temperatures $\tau_m = \tau_q = 0.1$. We utilize the pre-trained HuggingFace implementation of DistilBERT (Wolf et al., 2019). We set margin ψ as 0.4, 0.3, and 0.1 for Charades-STA, ActivityNet, and TACoS, respectively. We use AdamW (Loshchilov and Hutter, 2017) optimizer with learning rate of 1×10^{-4} , 8×10^{-4} , 1.5×10^{-3} for Charades-STA, ActivityNet, and TACoS, respectively. We set λ as 0.05 for Charades-STA and TACoS and 0.1 for ActivityNet. We set the reliable true-negatives filtering threshold $t_{tr} = 0.9$. We set the number of hard-negative samples to calculate $p'(q|v)$ as 100, 200, and 100 and $p'(v|q)$ as 50, 100, and 5 for Charades-STA, ActivityNet, and TACoS, respectively. The experimental results for various hyper-parameters for the hard-negative sampling are shown in Figure 8.

C.2 Baselines

MMN (Wang et al., 2022) adopts a dual-modal encoding design to get video clip and text representations. We utilized the publicly deployed code² to implement our own MMN model for our experiment using exactly the same hyper-parameters setting.

G2L (Li et al., 2023) uses a semantically aligned and uniform video grounding framework via

²<https://github.com/MCG-NJU/MMN>

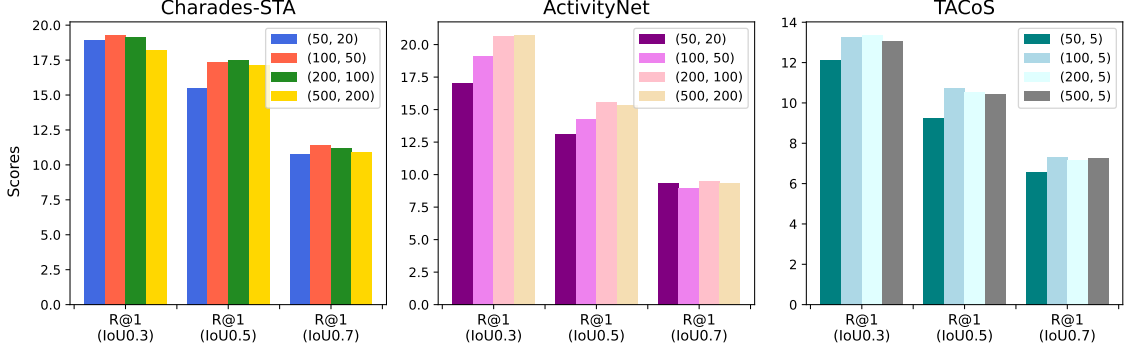


Figure 8: **Evaluation results for various hyper-parameters.** We search various hyper-parameters for the hard negative sampling. We measure R@1 (IoU>m), where $m \in \{0.3, 0.5, 0.7\}$ to find the best hyper-parameters. In this figure, each (x, y) means the number of negative samples. x and y mean a number of negative samples for $p'(v|q)$ (query-to-video) and $p'(q|v)$ (query-to-video), respectively. Consequently, we select the number of the CM-ANS samples to calculate $p'(q|v)$ as 100, 200, and 100 and $p'(v|q)$ as 50, 100, and 5 for Charades-STA, ActivityNet, and TACoS, respectively.

geodesic and game theory. We utilized the publicly deployed code³ to implement our own G2L model for our experiment using exactly the same hyper-parameters setting proposed by the paper.

Cross-Encoder Transformer (CET) is a cross-modal encoding model implemented based on a 6-layered transformer architecture. It is designed to predict the start and end points of a video moment by utilizing a model architecture, which is used in the QA task. We concatenate the pre-extracted video clip features and the text features derived from the Distil-BERT to use as an input of the transformer. To concatenate two extracted features, we should equalize the dimensions of two features with a linear layer as follows:

$$\begin{aligned}\bar{H}^v &= H^v W^v \\ \bar{H}^q &= H^q W^q\end{aligned}\quad (7)$$

where $H^v \in \mathbb{R}^{l_v, d^v}$, $H^q \in \mathbb{R}^{l_q, d^q}$, $W^v \in \mathbb{R}^{d^v, d}$, $W^q \in \mathbb{R}^{d^q, d}$. H^v is the pre-extracted video clip features and H^q is the features extracted using Distil-BERT. And then, we derive the representation of each video clip feature from the last layer of the transformer-encoder as follows:

$$H^{v,q} = \text{TransformerEnc}(\bar{H}^v \oplus \bar{H}^q) \quad (8)$$

where $H^{v,q} \in \mathbb{R}^{l_{vq}, d}$, $l_{vq} = l_v + l_q$. We utilize only the representation part of video features, and the 3-layered MLPs and Sigmoid follow them to predict the start and end positions of the moment, respectively, as follows:

$$\begin{aligned}p^s &= \text{Sigmoid}(\text{MLP}_s(H_{1:l_v}^{v,q})) \\ p^e &= \text{Sigmoid}(\text{MLP}_e(H_{1:l_v}^{v,q}))\end{aligned}\quad (9)$$

where p^s and $p^e \in \mathbb{R}^{l_v}$. We also introduce the interpolation labels y_i^s, y_i^e to utilize abundant information of moment labels as follows:

$$\begin{aligned}y_i^s &= \begin{cases} \left(\frac{x_e - i}{x_e^* - x_s^* + 1}\right)^k & \text{if } x_s^* \leq i \leq x_e^* \\ 0 & \text{otherwise} \end{cases} \\ y_i^e &= \begin{cases} \left(\frac{i - x_s}{x_e^* - x_s^* + 1}\right)^k & \text{if } x_s^* \leq i \leq x_e^* \\ 0 & \text{otherwise} \end{cases}\end{aligned}\quad (10)$$

We finally use the binary cross-entropy to calculate a loss for the pair of (p_i^s, y_i^s) and (p_i^e, y_i^e) as follows:

$$\begin{aligned}\mathcal{L}^s &= \text{BCE}(p^s, y^s) \\ \mathcal{L}^e &= \text{BCE}(p^e, y^e)\end{aligned}\quad (11)$$

where BCE means the binary cross-entropy. The final loss to train the CET model is defined as follows:

$$\mathcal{L} = \frac{\mathcal{L}^s + \mathcal{L}^e}{2} \quad (12)$$

We use $k = 10$ and $d = 512$ as a hyperparameter and AdamW optimizer with learning rate $1e-3$.

Bi-Encoder Transformer (BET) is a dual-modal encoding model that encodes text and video clip features independently. The pre-extracted video clip features are encoded using a 6-layered transformer, and text features are encoded using

³<https://github.com/lihxxxxx/G2L?tab=readme-ov-file>

the Distil-BERT, followed by the average-pooling function and 3-layered MLPs.

$$\tilde{H}^v = \text{TransformerEnc}(\bar{H}^v) \quad (13)$$

$$\begin{aligned} \tilde{H}^s &= \text{MLP}_s(\text{Pool}(\bar{H}^q)) \\ \tilde{H}^e &= \text{MLP}_e(\text{Pool}(\bar{H}^q)) \end{aligned} \quad (14)$$

Where $\tilde{H}^v \in \mathbb{R}^d$, $\tilde{H}^s \in \mathbb{R}^d$ and $\tilde{H}^e \in \mathbb{R}^d$. *Pool* means the average pooling. We calculate the cosine similarity between the encoded video clip representations and the encoded start and end representations to predict a moment.

$$\begin{aligned} p^s &= \text{Sigmoid}(r * \text{cosine}(\tilde{H}^v, \tilde{H}^s)) \\ p^e &= \text{Sigmoid}(r * \text{cosine}(\tilde{H}^v, \tilde{H}^e)) \end{aligned} \quad (15)$$

We use the interpolation labels and the binary cross-entropy loss for the BET, similar to CET. We use $r = 10$ and $d = 512$ as a hyperparameter and AdamW optimizer with learning rate 1e-3.

D Examples of False Negative Videos

Illustrative instances of constructed MVMR datasets can be found in Figure 9. This figure shows video instances that have been identified as similar to a specific target query. The target queries correspond to queries of Charades-STA, ActivityNet, and TACoS datasets, sequentially.

E Human Evaluation for the constructed MVMR Datasets

We conduct a human evaluation on our constructed MVMR datasets to reveal that our method construct MVMR datasets effectively. We recruit crowd workers fluent in English through the university’s online community. The recruited annotators were provided with a detailed description of task definitions, instructions. An example of a sheet we use to conduct a human evaluation is shown in Figure 10.

Query: person closes the door

Golden positive Moment: 26.2s ~ 31.3s

Filtered as positive # 1 Moment: 14.2s ~ 23.0s

Filtered as positive # 2 Moment: 25.2s ~ 30.0s

Original query: 'person closing the door.', 'person begins to undress.', ...

Original query: 'a person runs to the doorway of the pantry.', 'person closes the door.', ...

Filtered as negative # 1

Filtered as negative # 2

Filtered as negative # 3

Original query: 'person lies down on the bed to review the pictures.', 'taking the picture the person lies back in the bed.' 30.3s

Original query: 'person drinking from a glass of water.' 30.5s

Original query: 'another person comes running throwing open the door.' 30.7s

Query: A woman brushes and styles her hair.

Golden positive Moment: 1.1s ~ 86.7s

Filtered as positive # 1 Moment: 121.4s ~ 211.2s

Filtered as positive # 2 Moment: 11.6s ~ 14.1s

Original query: 'a woman hair is being sprayed by another woman.', 'then the woman's hair gets brushed.', ... 211.2s

Original query: 'A woman is brushing her hair.', 'She starts braiding her hair behind her head.', ... 166.0s

Filtered as negative # 1

Filtered as negative # 2

Filtered as negative # 3

Original query: 'A male chef appears in a kitchen standing...', 'The man then grabs the knife and starts...', ... 129.0s

Original query: 'A man is playing a game inside a court.', 'He talks to the camera bout the game.', ... 125.5s

Original query: 'A man is seen with his arm up and waves...', 'He then climbs up on a beam and begins...', ... 49.6s

Query: The person washed and dried their hands

Golden positive Moment: 131.8s ~ 136.5s

Filtered as positive # 1 Moment: 36.9s ~ 48.2s

Filtered as positive # 2 Moment: 234.7s ~ 241.7s

Original query: 'The person washes his hands with water...', 'The person got the cutting board out.', ... 89.5s

Original query: 'The person washes her hands.', 'She took out kiwi', ... 249.8s

Filtered as negative # 1

Filtered as negative # 2

Original query: 'He took out a second smaller glass', 'He cracked egg', ... 82.1s

Original query: 'He took out mango', 'He cut mango in half', ... 372.5s

Figure 9: **Examples of constructed MVMR datasets.** We visualize positive and negative video sets for the query “person closes the door” of three constructed datasets. A green solid box means a golden positive moment, and blue solid boxes show moments assigned to videos classified as positive. The underlined queries mean the most similar query described in Section 4.1 (*max aggregation*).

Name:

Start.

Is there any moment in the video that matches the text?

Yes ▼

If it exists, enter the moment. Leave blank if it does not exist. (Example) In the case of 3 seconds, input 3

Submit.

Next Task (->)

Previous Task (<-)

Enter the task number you want to move. (Ex) In the case of task 3, input 3.

Move.

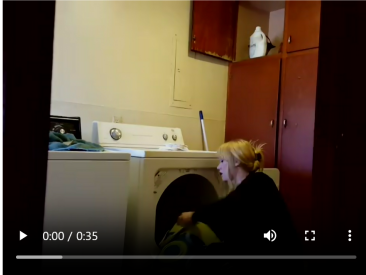
<Video-text matching Human Evaluation>

Login: yny

1. Task ID: 8

2. Text: person puts on shoes.

3. Video ID: J1MMG



0:00 / 0:35

Figure 10: **Human Evaluation Sheet Example.**